Computational and Theoretical Chemistry 1190 (2020) 113009

Contents lists available at ScienceDirect

Computational and Theoretical Chemistry

journal homepage: www.elsevier.com/locate/comptc

Insights on the mechanism, reactivity and selectivity of fructose and tagatose dehydration into 5-hydroxymethylfurfural: A DFT study

Lorena Maribel Meneses-Olmedo[a], Sebastián Cuesta Hoyos[a], Guillermo Salgado Moran[b], Wilson Cardona Villada[c], Lorena Gerli Candia[d], Luis H. Mendoza-Huizar[e,*]

[a] Laboratorio de Química Computacional, Facultad de Ciencias Exactas y Naturales, Pontificia Universidad Católica del Ecuador, Quito, Ecuador
[b] Facultad de Ciencias Físicas y Matemáticas, Universidad de Chile, Santiago, Chile
[c] Departamento de Ciencias Químicas, Facultad de Ciencias Exactas, Universidad Andrés Bello, Talcahuano, Chile
[d] Departamento de Química Ambiental, Facultad de Ciencias, Universidad Católica de la Santísima Concepción, Concepcion, Chile
[e] Universidad Autónoma del Estado de Hidalgo, Academic Area of Chemistry, Carretera Pachuca-Tulancingo Km. 4.5, Mineral de la Reforma, Hgo., Mexico

ARTICLE INFO

Keywords:
Biomass
Tagatose
Fructose
Tautomerization
Force quantum descriptor

ABSTRACT

In this study, a computational DFT study was performed to propose a new acid catalyzed mechanism to produce 5HMF from D-Fructose and D-Tagatose. The reactivity and selectivity towards 5HMF formation were analyzed, and the results revealed both saccharides present higher selectivity towards 5HMF with the first dehydration occurring on oxygen 2. Fructose seems to be more reactive than tagatose, although the dehydration process of the different hydroxyl groups on tagatose produces more unstable structures, which can undergo several side reactions. The new mechanism is proposed eliminating the tautomerization step and lowering the activation free energy of the second dehydration step in 21 kcal/mol.

1. Introduction

In the last decade, concerns about diminishing fossil fuel reserves and global warming caused by CO_2 emissions have increased interest in substituting oil, as a source of raw materials and energy, with environmentally friendly renewable resources [1–5]. In this sense, biomass is a promising alternative for producing oil derivatives as green fuels and chemicals and at the same time it allows to reduce the carbon footprint of some highly polluting industrial processes [2],[6,7],[8]. Moreover, biomass is abundant in carbon serving as a possible source of energy and organic compounds [9,10,11]. Nature is able to produce more than 200 billion tons of biomass, which is composed of more than 75% of carbohydrates [1],[11–13]. Therefore, converting the carbohydrates present in the biomass into fine chemicals is an enormous commercial potential [2],[12],[14]. Probably one of the main drawbacks, in the use of carbohydrates as a raw material, is the reactivity associated with the hydroxyl groups, which prevents an efficient selective conversion [12],[15],[16]. One way to perform selective chemistry of carbohydrates is to transform them into compounds containing a double bond C=C or a carbonyl group [12],. This will allow to induce different chemical reactions obtaining valuable chemicals with potential to manufacture plastics, rubbers, paper, pharmaceutical products, etc. [8],[11],[15],[17],[18].

In this sense, some monosaccharides (such as glucose and fructose), disaccharides (sucrose) and polymeric carbohydrates (starch, inulin and cellulose) can be used to produce 5 hydroxymethylfurfural (5HMF). 5HMF is a five-member multifunctional cyclic compound with high reactivity [6],[9],[11],[16],[19]. Note that 5HMF is a furan ring system with an alcohol group and an aldehyde group, where furan compounds can be used to produce polyurethanes, polyamides and polyesters as well as organic active ingredients [11],[14],[20].

5HMF is considered a high potential building block to produce bio-based organic molecules, fuels and materials replacing petroleum. It is in the US Department of Energýs "Top Value Added Chemicals" [1],[3], [4],[7],[8],[11],[16–18],[21],[22]. It was first described in the 19th century as a product of inulin and oxalic acid solution reaction under temperature and pressure [19],. It is obtained by the acid catalyzed dehydration of monosaccharides (hexoses) [1],[5],[6],[12],[15],[23], [24]. Here, it is important to mention that, nowadays this is the most promising process to use biomass as a source of fine chemicals. From 5HMF, other compounds such as liquid alkanes, levulinic acid, dimethylfuran, 2,5-Diformylfuran, 5-hydroxy-4-keto-2-pentenoic acid and 2,5-furandicarboxylic acid can be obtained to be used as fuels, pharmaceuticals and polymers [3],[5],[8],[12],[13],[16],[21],[22], [25],[26].

To efficiently produce 5HMF of monosaccharides, high temperature

* Corresponding author.
E-mail address: hhuizar@uaeh.edu.mx (L.H. Mendoza-Huizar).

https://doi.org/10.1016/j.comptc.2020.113009
Received 12 June 2020; Received in revised form 19 August 2020; Accepted 20 August 2020
Available online 26 August 2020
2210-271X/

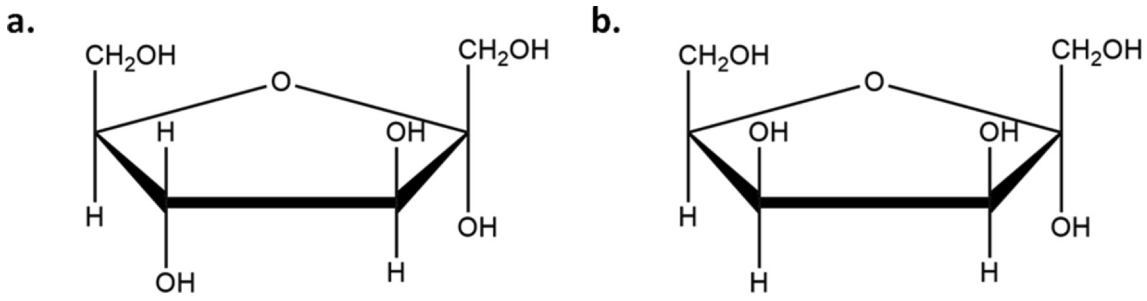

Fig. 1. Structure of (a) D-fructose (b) D-tagatose.

water is not enough. High pressure water (over 40 MPa), chromium salts in the presence of halide ions, PdAu/C catalyst, liquid mineral acids, including H_2SO_4, HCl and H_3PO_4, cation exchange resins, and different solvents have been used to produce 5HMF in high yields [3], [5–7],[10],[21],[27],[28]. Some studies on monosaccharides have determined that 5HMF can be produced selectively from keto-hexoses such as fructose instead from glucose [23],[26]. Even so, different yields of similar keto-hexoses have been obtained [5],[6],[13],[15], [20–22],[25],[27].

D-tagatose is a hexoketose, epimer of D-fructose (Fig. 1). It is present in small quantities in dairy products and in Sterculia setigera gum. Like other sugars, it is a white crystal or powder, very soluble in water and 90% as sweet as sucrose [29],[30].

Several computational studies based on DFT calculations have focused on elucidating the reaction mechanism of 5HMF production from glucose and fructose (Fig. 2) [1],[13],[18],[26]. For example, Li et al studied the reaction pathway for the dehydration of fructose into 5-hydroxymethylfurfural in the presence of BMImB, and they reported a mechanism with a barrier activation energy of 57 kcal mol^{-1}, of the rate-determining step [1], but this activation energy is at disagreement with the experimental results with a 95% 5HMF yield at 100 °C [26],. On the other hand, a DFT study of the fructose dehydration to 5-hydroxymethylfurfural catalyzed by 1-butyl-3-methyl-imidazolium bromide found an overall barrier of the catalytic conversion as 41.5 kcal mol^{-1} [26], which is more favorable that the previous mechanism reported by Li et al [1],. Thus, in order to find out a new mechanism that lowers the activation barrier to produce 5HMF, we performed a comparative computational study of an acid catalyzed reaction mechanism associated with the formation of 5HMF from fructose and tagatose to get a better understanding on the different dehydration steps Also, a reactivity and selectivity study is presented.

2. Computational methods

All the calculations were performed using Gaussian 16 software [31],. The initial fructose and tagatose structures were visualized employing Gaussview 05 [32], based on the three-dimensional structure reported in Drugbank [33], and Pubchem [34],. For the reaction mechanisms of 5HMF formation from fructose and tagatose, the structures of the reagent (R), intermediate (INT), transition State (TS), and product (P) were optimized. All the computational calculations were performed using the Head-Gordon long-range dispersion-corrected hybrid functional ωB97XD [35–38] with a 6-311++G(d,p) basis set. It has been reported that this level of theory is an effective choice that gives an accurate description of hydrogen transfer reactions and hydrogen-bonded species [39],. Frequency calculations were also performed in all structures to characterize each stationary point. For the TS, a negative frequency was associated with the changes occurring at that step of the reaction [40],. The Truhlar Universal Solvation Model Based on Solute Electron Density and on a Continuum Model of the Solvent Defined by the Bulk Dielectric Constant and Atomic Surface Tensions was used in the calculations. [41],[42].

For the monosaccharide protonation free energies (PE) study, the values were obtained using Eq. (1).

$$\Delta PE = (E_{(Protonatedstructure)} + E_{(H2O)}) - \left((E_{(monosacharide)} + E_{(H3O^+)}\right) \quad (1)$$

It is important to mention that protonation free energies involves different energetic contributions, due geometric and electronic rearrangements [43],. In this sense, a thermodynamic cycle should be considered to evaluate these energies when multiple tautomeric forms are present [44],. Nevertheless, in the case of the protonation free energies for fructose to 5HMF, similar procedures to that represented by Eq. (1) have been reported in the literature and the theoretical results obtained compare favorably with the experimental ones [26],[45], which suggests that the intrinsic error due to the simple description of hydronium and protonated species is canceled and confident results

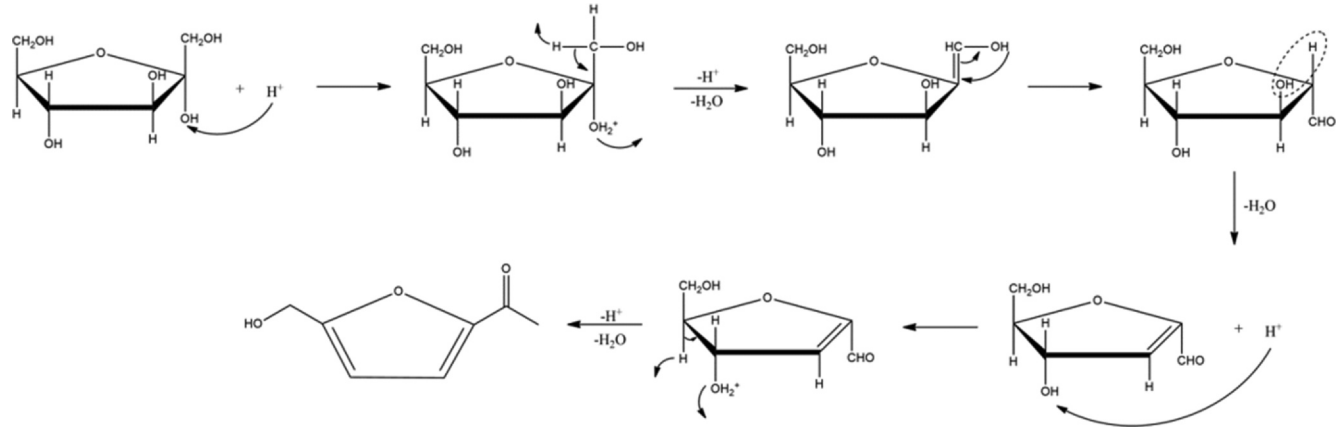

Fig. 2. Reported reaction mechanism to produce 5HMF from Fructose [1],[13],[18],[26].

may be obtained. The reaction profiles were constructed using free energy values obtained from each optimized structure. In order to describe and analyze each step of the reaction, an intrinsic reaction coordinate (IRC) calculation was performed, which allowed to obtain a view of the structural changes that occur in each step of the reaction [46,47],[48]. Here, it is convenient to mention that for any chemical process with energy profile E(ξ), along the reaction coordinate ξ, the reaction force F(ξ) is defined by Eq. (2) [49–55]:

$$F(\xi) = -\frac{dE}{d\xi} \tag{2}$$

This index is characterized by two critical points at ξ_i and ξ_j that provide a natural partitioning of the reaction coordinate into three regions, the reactant, transition state, and product regions [56],. Thus, in the reaction force profile, reaction "works" associated with electronical and geometrical changes in each step of the reaction mechanism can be obtained by integrating each part of the profile by using Eq. (3).

$$W_x = -\int_{\xi i}^{\xi j} F(\xi) d\xi \tag{3}$$

In a common one step reaction, four associated works (w) can be estimated where w1 and w4 belong to the geometrical contribution while w2 and w3 to the electronic ones. But, in a stepwise mechanism, 7 reaction works can be obtained where w1, w4 and w7 are attributed to structural changes and w2, w3, w5 and w6 to the electronic changes.

3. Results

For all the results obtained in the present work, carbon and oxygen atoms were labelled as shown in Fig. 3.

3.1. Reactivity and selectivity

In the first part of the study, the reactivity and selectivity of both monosaccharides (fructose and tagatose) were compared to analyze their selectivity to produce 5HFM. Thus, two sets of calculations were performed. In the first one, the selectivity was tested through a geometrical analysis, an NBO charge calculation and a free energy estimation (Δ*PE*) of the protonation process (Table 1) at each oxygen in both monosaccharides molecules. In an acidic aqueous environment, the equilibrium occurs between the saccharide and a hydronium ion (H_3O^+) as shown in Fig. 4. Here, in order to produce 5HMF, the reaction should start with the protonation at oxygen 2.

Results show that in acidic medium, the protonation of the oxygen atoms in fructose is a favorable process, except at oxygen 3 (0.3 kcal/mol). Thus, the order of protonation of the oxygen atoms is 6 < 2 < 4 < 5 < 1. On the other hand, the protonation of tagatose at any oxygen atom is a favorable process with negative Δ*PE* values in the range −3.2 to −0.2 kcal/mol. In this sense, the protonation of oxygen atoms, 1, 6 and 2 should be the most favorable in that order. Comparing the protonation of fructose and tagatose at O2, the Δ*PE* was lower in fructose by 0.5 kcal/mol. Comparing the protonation energy of the atoms, O4, O5, and O6 are easily protonated in Fructose while O1 and O3 in Tagatose.

Table 1
Free energy of the protonation process of the hydroxyl group in fructose and tagatose.

Protonated Oxygen	Δ*PE* in kcal/mol	
	Fructose	Tagatose
1	−2.6	−3.2
2	−3.3	−2.8
3	0.3	−0.2
4	−3.2	−1.8
5	−3.1	−2.4
6	−4.4	−3.0

A further geometrical characterization was performed to get an insight on this protonation process (not shown). The protonated structures were optimized, and different distances were measured to determine changes when the hydrogen atom protonates the oxygen. Analyzing oxygen-hydrogen distances, a negligible distance increase between 0.00 Å and 0.04 Å was observed. On the other hand, when analyzing the carbon oxygen distance, a bigger increase in the distance was found. In all the protonated oxygen, the change in the C—O distance was around 0.06 Å except for O2. When O2 is protonated, the C—O distance doubled increasing 0.15 Å for fructose and 0.14 Å for tagatose. Also, a NBO charge analysis was done to get an insight on the results obtained (Table 2).

Charges tabulated in Table 2 show C2 is the most acidic carbon in the molecule becoming an electrophilic center δ^+ (0.535 in fructose and 0.542 in tagatose). This occurs because it is surrounded by electron pulling groups. For C2; O2, O5 and the H_2C_2OH group are pulling electrons while for the other carbon atoms, only the contiguous oxygen can pull some electronic density. This makes C2-O2 bond the weakest. When O2 is protonated, the C2-O2 bond is almost lost making it easy for the water molecule to leave the system. When protonating the other oxygen atoms in the molecules, the bond enlarges a little but keeps stable. Therefore, for both fructose and tagatose, selectivity towards 5HMF formation was found.

Then, to see which of those protonated oxygen atoms can leave the system, creating side reactions (reactivity), scan calculations of the dehydration process at each oxygen atom after the protonation was investigated. From the scan plot (Energy vs C—O distance), the lowest energy value was set to zero (starting point). Distance and energy values at the most energetic point were tabulated in Table 3.

Table 3 shows that the dehydration process of O2 is the least energetic one (~2.5 kcal/mol) being in agreement with the previous results. Dehydration in positions 1 and 4 presents a similar energy for fructose and tagatose. A difference in the dehydration process in position 3 and 6 was found. In both positions, the dehydration process is favored for fructose having a lower activation energy (9.5 kcal/mol

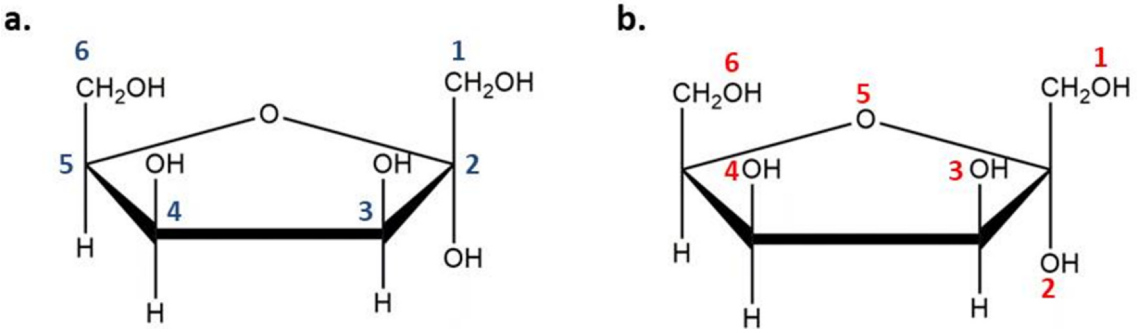

Fig. 3. Saccharides carbon (b) and oxygen (a) labelling.

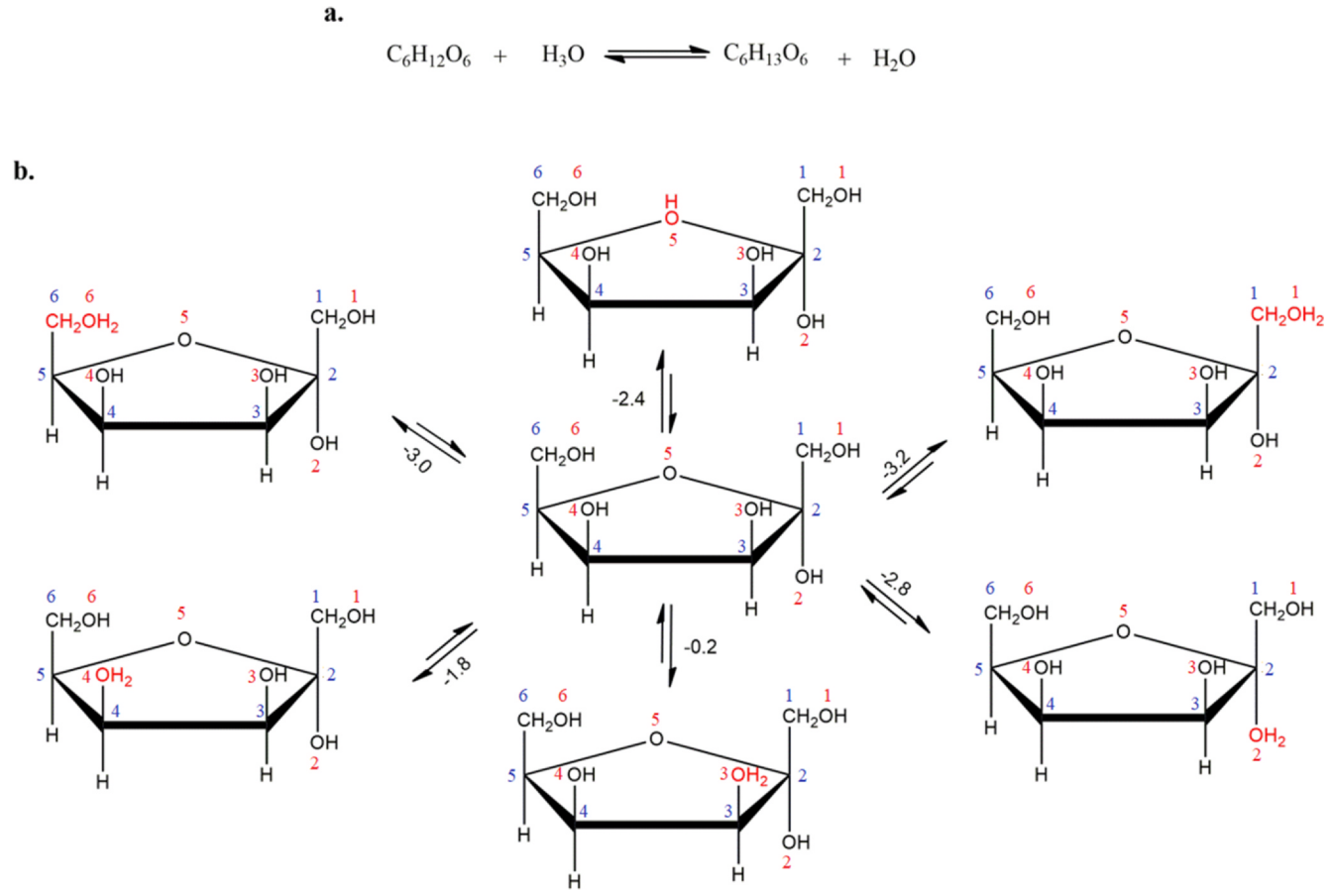

Fig. 4. (a) Reaction equilibrium for the protonation process in hexoses. (b) protonation equilibrium at every hydroxyl group in tagatose. Energies in kcal/mol.

Table 2
NBO charges of carbon and oxygen atoms in fructose and tagatose.

Atom	Fructose		Tagatose	
	C	*O*	*C*	*O*
1	−0.055	−0.776	−0.063	−0.777
2	0.535	−0.798	0.542	−0.782
3	0.071	−0.775	0.072	−0.775
4	0.078	−0.781	0.088	−0.788
5	0.080	−0.659	0.088	−0.663
6	−0.049	−0.782	−0.046	−0.789

Table 3
Carbon–Oxygen distance for the dehydration process of fructose and tagatose.

Protonated Oxygen	Fructose			Tagatose		
	Starting Distance (Å)	End Distance (Å)	Free energy (kcal/mol)	Starting Distance (Å)	End Distance (Å)	Free energy (kcal/mol)
1	1.48	2.30	35.5	1.48	2.34	37.5
2	1.57	2.05	2.6	1.55	1.97	2.5
3	1.49	2.27	27.1	1.47	2.23	36.6
4	1.48	2.36	29.5	1.48	2.76	29.5
6	1.50	2.62	32.5	1.48	2.78	40.0

lower in position 3 and 7.5 kcal/mol for position 6). This suggests that in the dehydration process, fructose seems to be more reactive than tagatose. Analyzing more in depth position 4, the dehydration process in fructose produces a more stable structure as the hydroxyl group in position 3 moves towards C4. On the other hand, in tagatose, as the water molecule leaves the systems, steric effects prevent the hydroxyl group in position 3 to stabilize the molecule. This may cause more side reactions to occur (Fig. 5). The same occurs in the dehydration process at position 6, where there is a ring opening as the water molecule leaves the system. Thus, the *trans* conformation in fructose stabilizes the molecule being less reactive than tagatose.

3.2. Reaction mechanism

Tagatose reaction mechanism (Fig. 6) was proposed and studied based on the reaction mechanism for the fructose transformation into 5HMF (Fig. 2) reported by De Melo et al. [2],.

The reaction profile of the mechanism for fructose and tagatose depicted in Fig. 6 is presented in Fig. 7 and the activation energies in Table 4. In steps having more than one transition state, only the rate determining step was tabulated.

It is clear that in the reaction mechanism depicted in Fig. 6, the rate determining step is the tautomerization process, with an activation energy of ~60 kcal/mol. However, a mechanism with a determining step of 60 kcal/mol barrier will never occur because it corresponds to a rate constant of practically zero (if the reaction is unimolecular, like the tautomerization), last result contrast with the high yields of 5HMF obtained experimentally [3],[5–7],[10],[21],[27],[28]. The second most energetic process is dehydration 2. The first dehydration comprises a stepwise mechanism where, in the first part, the protonated hydroxyl group in position 2 leaves the system as a water molecule followed by the deprotonation of a hydrogen atom in C1 (Fig. 8).

The IRC plot for both saccharides indicates a very similar profile. This was expected as the atoms involve in this step are the same in both molecules with little influence of position 4 (where OH position is

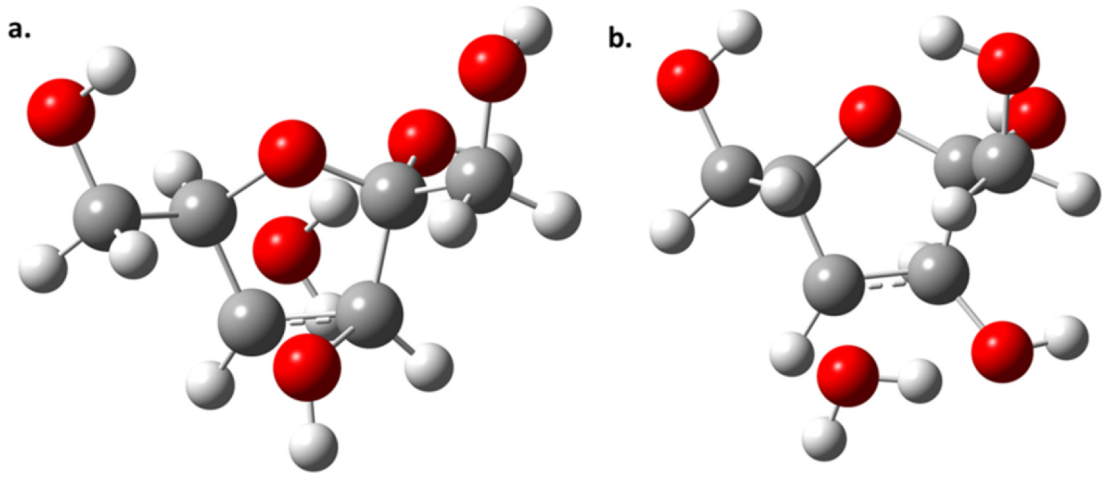

Fig. 5. Dehydration process of fructose (a) and tagatose (b) at position 4.

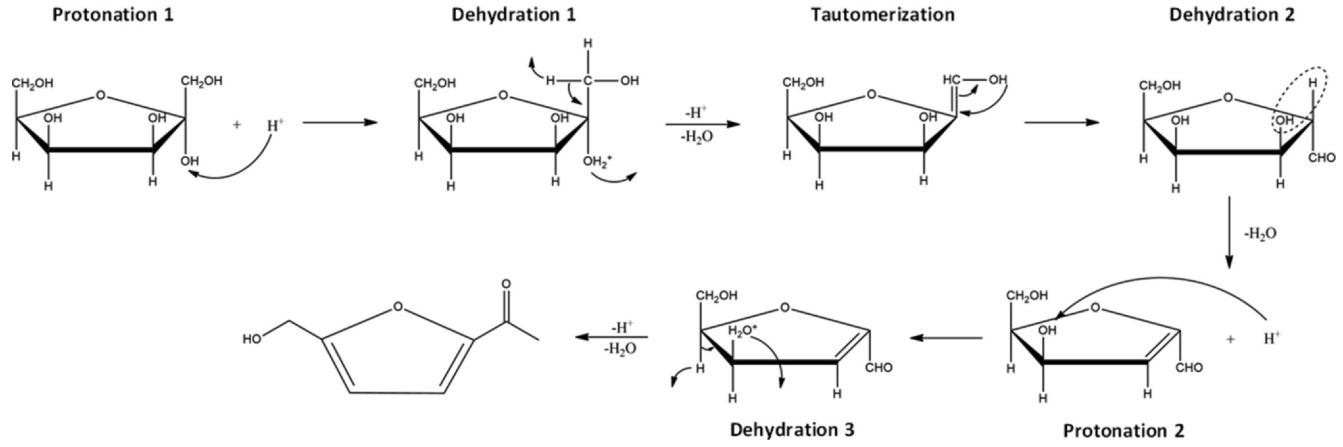

Fig. 6. Reaction mechanism to produce 5HMF from Tagatose based on the reaction mechanism reported by De Melo et al. [2],.

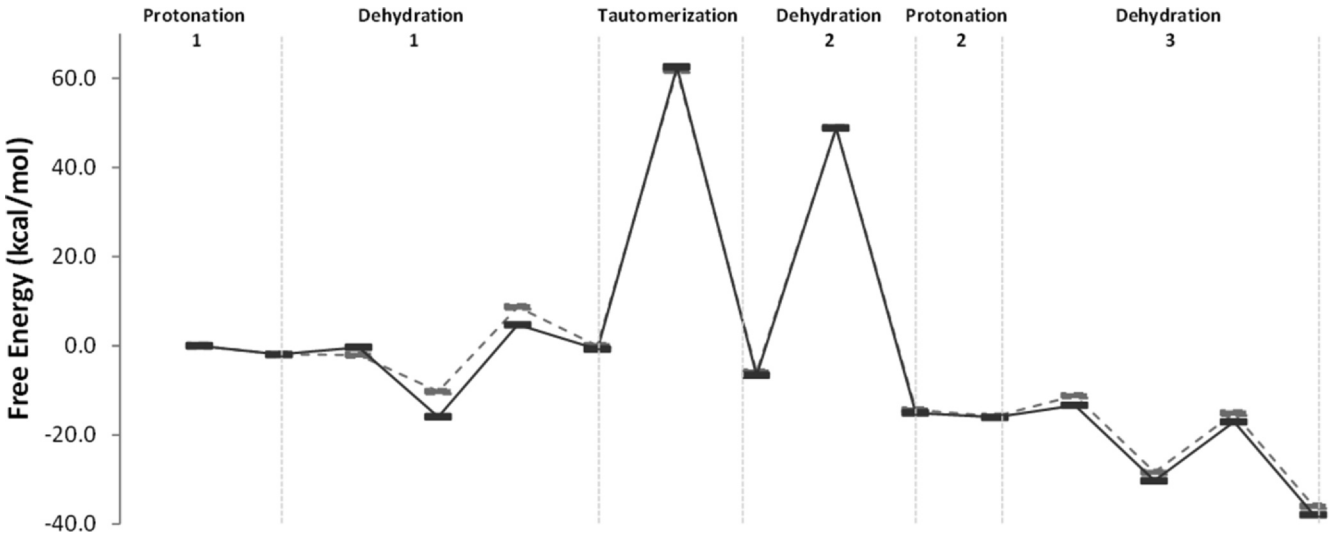

Fig. 7. Reaction profile for fructose (dotted line) and tagatose (solid line) for the reaction mechanism based on the mechanism reported by De Melo et al. [2], and calculated in this work at the ωB97xd/6-311 + + G(d,p) level of theory.

different). The same can be observed in the tautomerization step where the proton in O1 is transferred to C2 (Fig. 9). In this case, both profiles are identical.

In the second dehydration step (Fig. 10), the hydrogen of C2 bonds to O3 forming a water molecule that leaves the system. Note that this mechanism should be occur through a concerted mechanism, although a shoulder can be seen indicating a small stabilization of the structure (barrier less process). In this step, the proton is transferred from the carbon to the oxygen and then the water molecule formed leaves the system.

Table 4
Activation energy of the different steps in 5HMF formation.

Step	Activation free energy (kcal/mol)	
	Fructose	Tagatose
Dehydration 1	19.0	20.7
Tautomerization	61.8	63.3
Dehydration 2	54.7	55.1
Dehydration3	13.2	13.2

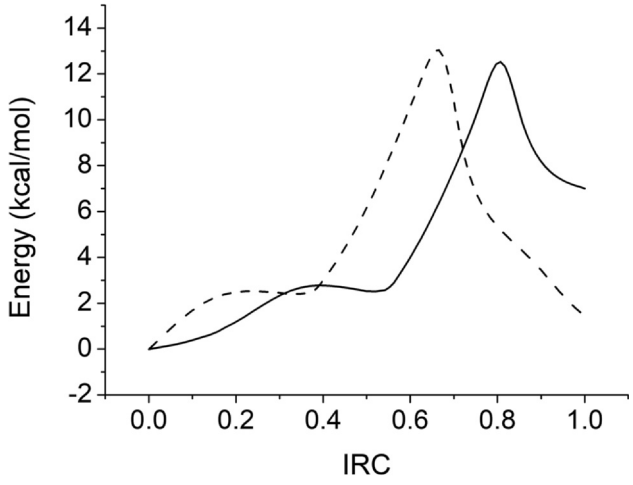

Fig. 8. IRC profile of the first dehydration step for fructose (dotted line) and tagatose (solid line) according to the mechanism depicted in Fig. 6.

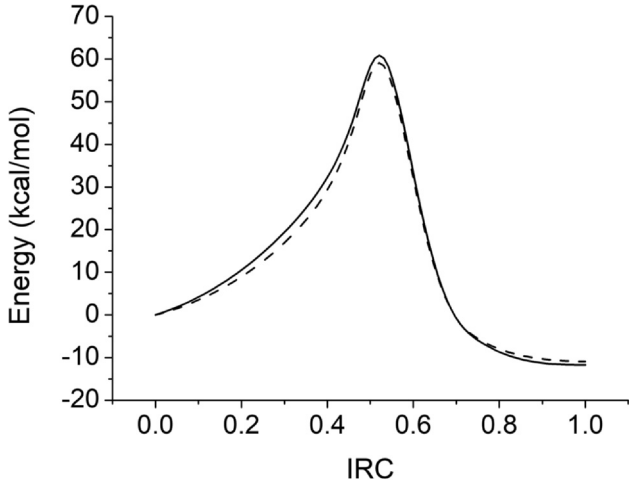

Fig. 9. IRC profile of the tautomerization step for fructose (dotted line) and tagatose (solid line) according to the mechanism depicted in Fig. 6.

Probably, the third dehydration step (Fig. 11) is the important one because is where the difference between fructose and tagatose may be observed. For this step to happen, a second external protonation (in this case of O4) occurs. Although the IRC profiles are similar, it is clearly seen that the activation energy of the first step which includes the water elimination is higher in fructose than in tagatose (2 kcal/mol). The second step is the same for both molecules leaving the final product 5HMF.

For a second dehydration process of the mechanism depicted in Fig. 6, a different option was tested to find a more favorable mechanism. Instead of a tautomerization followed by a proton transfer and a water elimination process, a direct proton transfer from O1 to O3 was tested. The energy estimated for this mechanism was 34.30 kcal/mol.

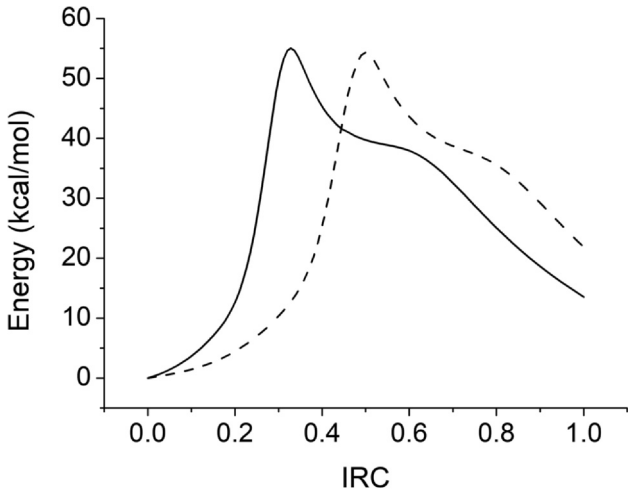

Fig. 10. IRC profile of the second dehydration step for fructose (dotted line) and tagatose (solid line).

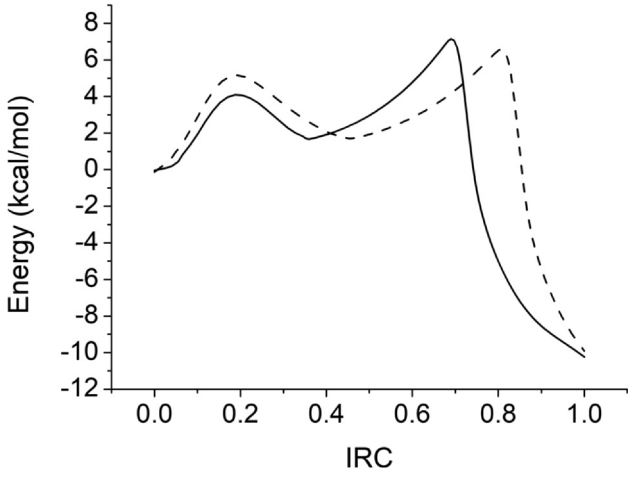

Fig. 11. IRC profile of the third dehydration step for fructose (dotted line) and tagatose (solid line).

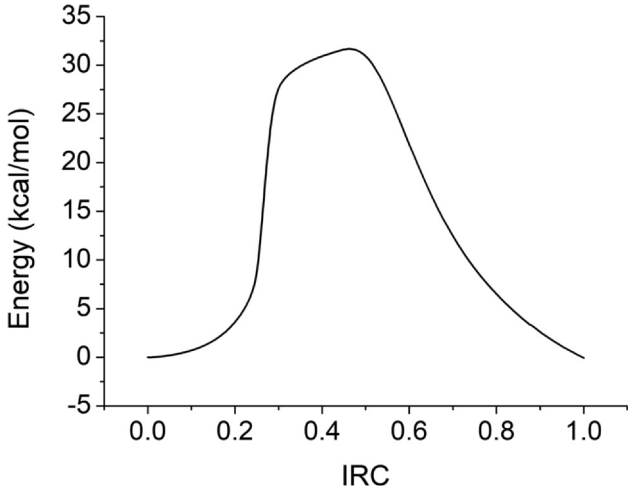

Fig. 12. IRC profile of a direct second dehydration process for tagatose proposed in the present work.

The IRC profile indicates a concerted mechanism causing the second dehydration to occur in a single energy favored step (Fig. 12).

Based on the last results, a new mechanism is proposed as shown in

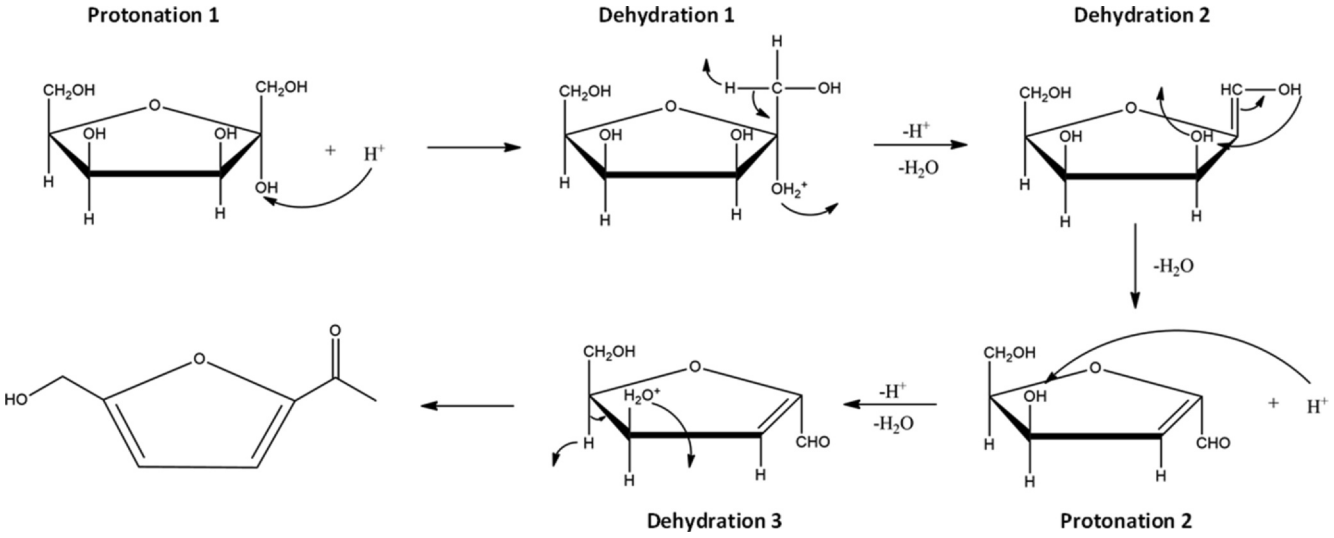

Fig. 13. New proposed reaction mechanism to produce 5HMF from Tagatose.

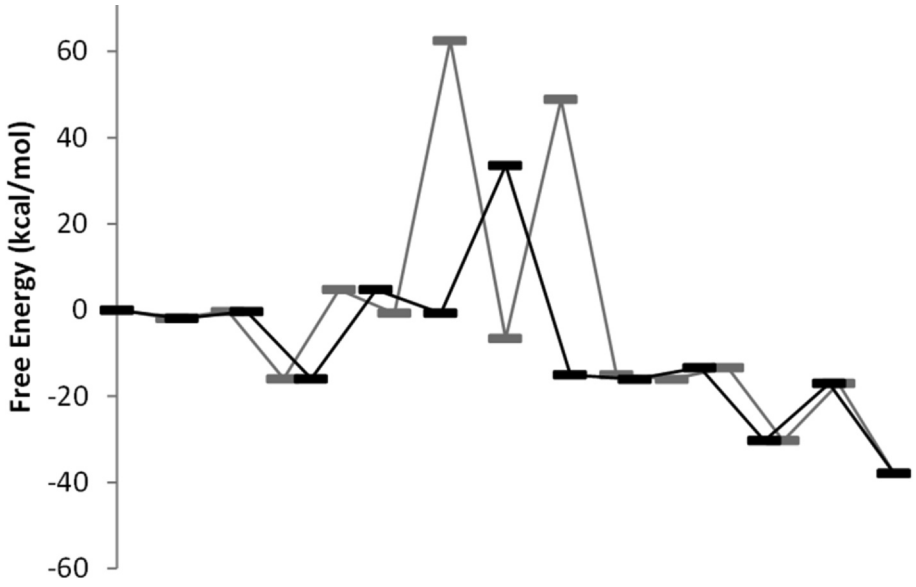

Fig. 14. Comparison of the reaction profile of tagatose. Grey lines indicate the mechanism based on the mechanism reported by De Melo et al. [2], and black lines the new one proposed, both profiles were calculated at the ωB97xd/6-311 + + G(d,p) level of theory.

Fig. 13, and its mechanism plotted and compared with the previous one in Fig. 14.

On the new proposed mechanism, the reaction force descriptor was applied at each step and plotted in Fig. 15.

In stepwise mechanisms such as the first and the third dehydration of the new mechanism (see Fig. 13), five zones were identified; reagent region (R → ξ1), transition state 1 region (ξ1 → ξ2), intermediate region (ξ2 → ξ3), transition state 2 region (ξ3 → ξ4) and product region (ξ4 → P). From those, seven reaction works were estimated. On the other hand, for concerted mechanisms such as the second dehydration process, three zones were identified; reagent region (R → ξ1), transition state region (ξ1 → ξ2), and product region (ξ2 → P) where only four reaction works were obtained (Table 5).

For the first dehydration process of the new mechanism, to reach the first transition state, the geometry changes contribute to 62% of the energy needed, while the electronic changes 38%. After the water molecule leaves the system, there is an important electronic rearrangement (9.9 kcal/mol). In the second step of the reaction, to get to the second transition state, structural changes contribute to 85% and electronic changes only 15%. In the second dehydration process, geometrical and electronical changes contribute almost half and half (51% for geometrical and 49% for electronical). This is due to the charge rearrangement happening in the entire furan ring after the proton leaves O1 and the hydroxyl group C3. The same contribution was found in the first step in the third dehydration process. For the second step, 86% of the contribution is made by geometrical changes and 14% by electronic ones

4. Conclusions

An acid catalyzed mechanism to produce 5HMF from D-Fructose and D-Tagatose was proposed where the tautomerization step is omitted and a direct proton transfer from O1 to O3 occurs. This process lowers the activation energy of the rate determining step in 29 kcal/mol in comparison with the reaction mechanism previously reported. The new proposed mechanism was studied using the reaction force formalism where it was found that electronic changes and geometrical changes have almost the same contribution in the second dehydration and in the

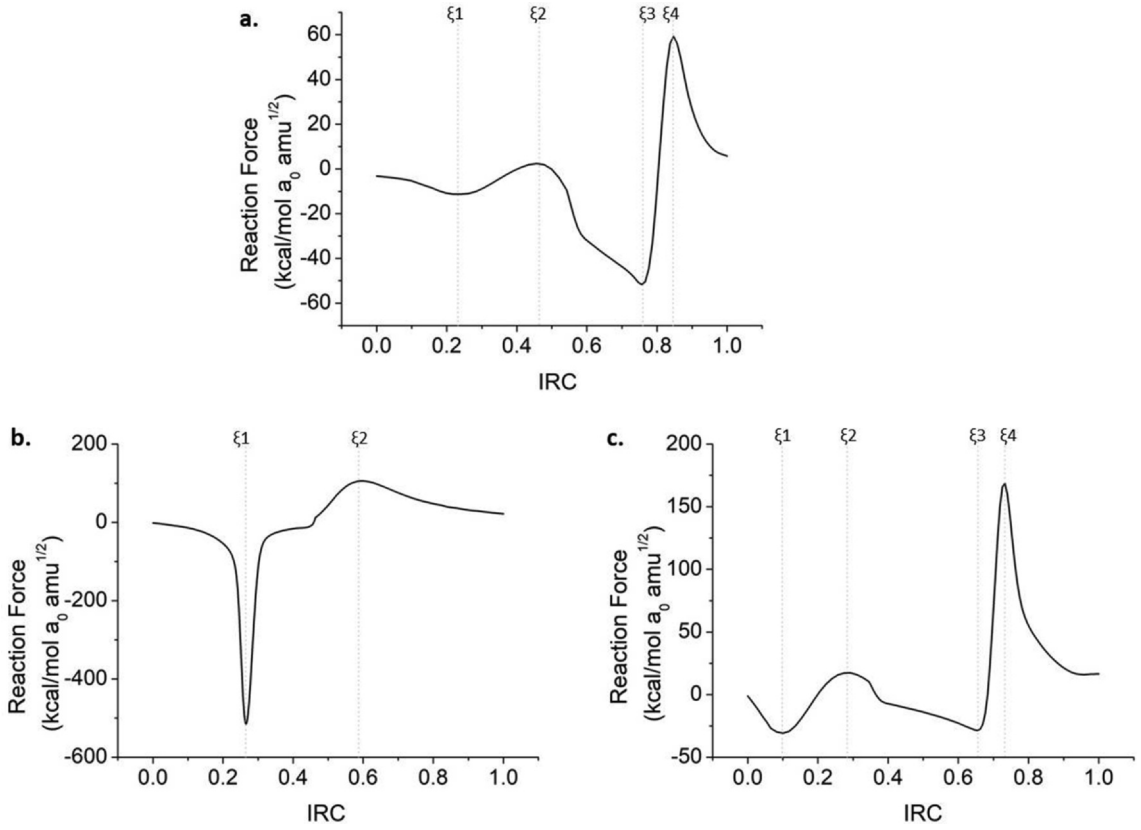

Fig. 15. Reaction Force profile of the first (a), Second (b) and third (c) dehydration process of tagatose towards 5HMF.

Table 5
Reaction work (kcal/mol) for the different dehydration processes of Tagatose.

Step	W1	W2	W3	W4	W5	W6	W7
1st	1.7	1.0	9.9	8.3	1.4	−1.9	−3.5
2nd	16.2	15.5	−9.6	−21.9	–	–	–
3rd	1.9	1.8	−1.1	3.6	0.6	−4.9	−12.1

first step of dehydration 1 and 3. This is due to all the electronic rearrangements that have to happen in the furan ring every time a hydroxyl group leaves the system. For the second step in the first and third dehydration, geometrical changes account for 85% of the contribution while electronic only 15%.

CRediT authorship contribution statement

Lorena Maribel Meneses-Olmedo: Conceptualization, Methodology, Writing - original draft, Data curation, Software, Writing - review & editing. **Sebastián Cuesta Hoyos:** Conceptualization, Methodology, Writing - original draft, Data curation, Software, Writing - review & editing. **Guillermo Salgado Moran:** Conceptualization, Investigation, Writing - original draft, Writing - review & editing. **Wilson Cardona Villada:** Methodology, Data curation, Software, Writing - review & editing. **Lorena Gerli Candia:** Visualization, Investigation, Validation, Writing - review & editing. **Luis H. Mendoza-Huizar:** Conceptualization, Investigation, Writing - original draft, Writing - review & editing.

Declaration of Competing Interest

The authors declare that they have no known competing financial interests or personal relationships that could have appeared to influence the work reported in this paper.

Acknowledgement

LHMH gratefully acknowledges financial support from CONACYT (project CB-2015-257823) and to the Universidad Autónoma del Estado de Hidalgo. Guanajuato National Laboratory (CONACyT 123732) is acknowledged for supercomputing resources. LHMH acknowledges to the SNI for the distinction of his membership and the stipend received.

References

[1] Y.N. Li, J.Q. Wang, L.N. He, Z.Z. Yang, A.H. Liu, B. Yu, C.R. Luan, Experimental and theoretical studies on imidazolium ionic liquid-promoted conversion of fructose to 5-hydroxymethylfurfural, Green Chem. 14 (2012) 2752–2758, https://doi.org/10.1039/c2gc35845j.
[2] F.C. De Melo, R.F. De Souza, P.L.A. Coutinhob, M.O. De Souza, Synthesis of 5-Hydroxymethylfurfural from dehydration of fructose and glucose using ionic liquids, J. Braz. Chem. Soc. 25 (2014) 2378–2384, https://doi.org/10.5935/0103-5053.20140256.
[3] A. Osatiashtiani, A.F. Lee, D.R. Brown, J.A. Melero, G. Morales, K. Wilson, Bifunctional SO4/ZrO2 catalysts for 5-hydroxymethylfufural (5-HMF) production from glucose, Catal. Sci. Technol. 4 (2014) 333–342, https://doi.org/10.1039/c3cy00409k.
[4] X. Qi, M. Watanabe, T.M. Aida, R.L. Smith, Catalytic dehydration of fructose into 5-hydroxymethylfurfural by ion-exchange resin in mixed-aqueous system by microwave heating, Green Chem. 10 (2008) 799–805, https://doi.org/10.1039/b801641k.
[5] S. Nishimura, N. Ikeda, K. Ebitani, Selective hydrogenation of biomass-derived 5-hydroxymethylfurfural (HMF) to 2,5-dimethylfuran (DMF) under atmospheric hydrogen pressure over carbon supported PdAu bimetallic catalyst, Catal. Today (2014) 89–98, https://doi.org/10.1016/j.cattod.2013.10.012 Elsevier.
[6] J.B. Binder, A.V. Cefali, J.J. Blank, R.T. Raines, Mechanistic insights on the conversion of sugars into 5- hydroxymethylfurfural, Energy Environ. Sci. 3 (2010) 765–771, https://doi.org/10.1039/b923961h.
[7] F. Guo, Z. Fang, T.J. Zhou, Conversion of fructose and glucose into 5-hydroxymethylfurfural with lignin-derived carbonaceous catalyst under microwave irradiation in dimethyl sulfoxide-ionic liquid mixtures, Bioresour. Technol. 112 (2012) 313–318, https://doi.org/10.1016/j.biortech.2012.02.108.
[8] R. Kourieh, V. Rakic, S. Bennici, A. Auroux, Relation between surface acidity and reactivity in fructose conversion into 5-HMF using tungstated zirconia catalysts, Catal. Commun. 30 (2013) 5–13, https://doi.org/10.1016/j.catcom.2012.10.005.

[9] W. Mamo, Y. Chebude, C. Márquez-Álvarez, I. Díaz, E. Sastre, Comparison of glucose conversion to 5-HMF using different modified mordenites in ionic liquid and biphasic media, Catal. Sci. Technol. 6 (2016) 2766–2774, https://doi.org/10.1039/c5cy02070k.

[10] Y. Qu, C. Huang, J. Zhang, B. Chen, Efficient dehydration of fructose to 5-hydroxymethylfurfural catalyzed by a recyclable sulfonated organic heteropolyacid salt, Bioresour. Technol. 106 (2012) 170–172, https://doi.org/10.1016/j.biortech.2011.11.069.

[11] M.E. Zakrzewska, E. Bogel-Łukasik, R. Bogel-Łukasik, Ionic liquid-mediated formation of 5-hydroxymethylfurfural-A promising biomass-derived building block, Chem. Rev. 111 (2011) 397–417, https://doi.org/10.1021/cr100171a.

[12] M. Bicker, J. Hirth, H. Vogel, Dehydration of fructose to 5-hydroxymethylfurfural in sub-and supercritical acetone, Green Chem. 5 (2003) 280–284, https://doi.org/10.1039/b211468b.

[13] R.J. Van Putten, J.N.M. Soetedjo, E.A. Pidko, J.C. Van Der Waal, E.J.M. Hensen, E. De Jong, H.J. Heeres, Dehydration of different ketoses and aldoses to 5-hydroxymethylfurfural, ChemSusChem. 6 (2013) 1681–1687, https://doi.org/10.1002/cssc.201300345.

[14] X. Qi, M. Watanabe, T.M. Aida, R.L. Smith, Catalytical conversion of fructose and glucose into 5-hydroxymethylfurfural in hot compressed water by microwave heating, Catal. Commun. 9 (2008) 2244–2249, https://doi.org/10.1016/j.catcom.2008.04.025.

[15] T.S. Hansen, J.M. Woodley, A. Riisager, Efficient microwave-assisted synthesis of 5-hydroxymethylfurfural from concentrated aqueous fructose, Carbohydr. Res. 344 (2009) 2568–2572, https://doi.org/10.1016/j.carres.2009.09.036.

[16] H. Zhao, J.E. Holladay, H. Brown, Z.C. Zhang, Metal chlorides in ionic liquid solvents convert sugars to 5-hydroxymethylfurfural, Science (80-.) 316 (2007) 1597–1600, https://doi.org/10.1126/science.1141199.

[17] Z. Zhang, B. Liu, Z. Zhao, Conversion of fructose into 5-HMF catalyzed by GeCl 4 in DMSO and [Bmim]Cl system at room temperature, Carbohydr. Polym. 88 (2012) 891–895, https://doi.org/10.1016/j.carbpol.2012.01.032.

[18] G. Yang, E.A. Pidko, E.J.M. Hensen, Mechanism of Bronsted acid-catalyzed conversion of carbohydrates, J. Catal. 295 (2012) 122–132, https://doi.org/10.1016/j.jcat.2012.08.002.

[19] A.A. Rosatella, S.P. Simeonov, R.F.M. Frade, C.A.M. Afonso, 5-Hydroxymethylfurfural (HMF) as a building block platform: biological properties, synthesis and synthetic applications, Green Chem. 13 (2011) 754–793, https://doi.org/10.1039/c0gc00401d.

[20] C. Moreau, R. Durand, S. Razigade, J. Duhamet, P. Faugeras, P. Rivalier, R. Pierre, G. Avignon, Dehydration of fructose to 5-hydroxymethylfurfural over H-mordenites, Appl. Catal. A Gen. 145 (1996) 211–224, https://doi.org/10.1016/0926-860X(96)00136-6.

[21] X. Qi, M. Watanabe, T.M. Aida, R.L. Smith, Efficient process for conversion of fructose to 5-hydroxymethylfurfural with ionic liquids, Green Chem. 11 (2009) 1327–1331, https://doi.org/10.1039/b905975j.

[22] R.J. van Putten, J.C. van der Waal, E. de Jong, H.J. Heeres, Reactivity studies in water on the acid-catalysed dehydration of psicose compared to other ketohexoses into 5-hydroxymethylfurfural, Carbohydr. Res. 446–447 (2017) 1–6, https://doi.org/10.1016/j.carres.2017.04.009.

[23] B.F.M. Kuster, 5-Hydroxymethylfurfural (HMF). A review focussing on its manufacture, Starch - Stärke 42 (1990) 314–321, https://doi.org/10.1002/star.19900420808.

[24] M.J. Taherzadeh, L. Gustafsson, C. Niklasson, G. Lidén, Physiological effects of 5-hydroxymethylfurfural on Saccharomyces cerevisiae, Appl. Microbiol. Biotechnol. 53 (2000) 701–708, https://doi.org/10.1007/s002530000328.

[25] R.J. van Putten, J.C. van der Waal, M. Harmse, H.H. van de Bovenkamp, E. de Jong, H.J. Heeres, A comparative study on the reactivity of various Ketohexoses to Furanics in methanol, ChemSusChem. 9 (2016) 1827–1834, https://doi.org/10.1002/cssc.201600252.

[26] J. Li, Y. Yang, D. Zhang, DFT study of fructose dehydration to 5-hydroxymethylfurfural catalyzed by imidazolium-based ionic liquid, Chem. Phys.Lett. 723 (2019) 175–181, https://doi.org/10.1016/j.cplett.2019.03.047.

[27] T.M. Aida, K. Tajima, M. Watanabe, Y. Saito, K. Kuroda, T. Nonaka, H. Hattori, R.L. Smith, K. Arai, Reactions of d-fructose in water at temperatures up to 400 °C and pressures up to 100 MPa, J. Supercrit. Fluids. 42 (2007) 110–119, https://doi.org/10.1016/j.supflu.2006.12.017.

[28] X. Qi, M. Watanabe, T.M. Aida, R.L. Smith, Sulfated zirconia as a solid acid catalyst for the dehydration of fructose to 5-hydroxymethylfurfural, Catal. Commun. 10 (2009) 1771–1775, https://doi.org/10.1016/j.catcom.2009.05.029.

[29] Y. Lu, G.V. Levin, T.W. Donner, Tagatose, a new antidiabetic and obesity control drug, Diab. Obes. Metab. 10 (2008) 109–134, https://doi.org/10.1111/j.1463-1326.2007.00799.x.

[30] D.K. Oh, Tagatose: properties, applications, and biotechnological processes, Appl. Microbiol. Biotechnol. 76 (2007) 1–8, https://doi.org/10.1007/s00253-007-0981-1.

[31] M.J. Frisch, G.W. Trucks, H.B. Schlegel, G.E. Scuseria, M.A. Robb, J.R. Cheeseman, G. Scalmani, V. Barone, G.A. Petersson, H. Nakatsuji, X. Li, M. Caricato, A. V Marenich, J. Bloino, B.G. Janesko, R. Gomperts, B. Mennucci, H.P. Hratchian, J. V Ortiz, A.F. Izmaylov, J.L. Sonnenberg, Williams, F. Ding, F. Lipparini, F. Egidi, J. Goings, B. Peng, A. Petrone, T. Henderson, D. Ranasinghe, V.G. Zakrzewski, J. Gao, N. Rega, G. Zheng, W. Liang, M. Hada, M. Ehara, K. Toyota, R. Fukuda, J. Hasegawa, M. Ishida, T. Nakajima, Y. Honda, O. Kitao, H. Nakai, T. Vreven, K. Throssell, J.A. Montgomery Jr., J.E. Peralta, F. Ogliaro, M.J. Bearpark, J.J. Heyd, E. N. Brothers, K.N. Kudin, V.N. Staroverov, T.A. Keith, R. Kobayashi, J. Normand, K. Raghavachari, A.P. Rendell, J.C. Burant, S.S. Iyengar, J. Tomasi, M. Cossi, J.M. Millam, M. Klene, C. Adamo, R. Cammi, J.W. Ochterski, R.L. Martin, K. Morokuma, O. Farkas, J.B. Foresman, D.J. Fox, Gaussian 16 Rev. B.01, 2016.

[32] R. Dennington, T. Keith, J. Millam, Gaussview, Version 5., 2016.

[33] D.S. Wishart, Y.D. Feunang, A.C. Guo, E.J. Lo, A. Marcu, J.R. Grant, T. Sajed, D. Johnson, C. Li, Z. Sayeeda, N. Assempour, I. Iynkkaran, Y. Liu, A. MacIejewski, N. Gale, A. Wilson, L. Chin, R. Cummings, Di. Le, A. Pon, C. Knox, M. Wilson, DrugBank 5.0: a major update to the DrugBank database for 2018, Nucl. Acids Res. 46 (2018) D1074–D1082, https://doi.org/10.1093/nar/gkx1037.

[34] S. Kim, J. Chen, T. Cheng, A. Gindulyte, J. He, S. He, Q. Li, B.A. Shoemaker, P.A. Thiessen, B. Yu, L. Zaslavsky, J. Zhang, E.E. Bolton, PubChem 2019 update: improved access to chemical data, Nucl. Acids Res. 47 (2019) D1102–D1109, https://doi.org/10.1093/nar/gky1033.

[35] S. Grimme, Semiempirical GGA-type density functional constructed with a long-range dispersion correction, J. Comput. Chem. 27 (2006) 1787–1799, https://doi.org/10.1002/jcc.20495.

[36] J. Da Chai, M. Head-Gordon, Systematic optimization of long-range corrected hybrid density functionals, J. Chem. Phys. 128 (2008) 84106, https://doi.org/10.1063/1.2834918.

[37] J. Da Chai, M. Head-Gordon, Long-range corrected hybrid density functionals with damped atom-atom dispersion corrections, PCCP 10 (2008) 6615–6620, https://doi.org/10.1039/b810189b.

[38] R. Nasiri, M.J. Field, M. Zahedi, A.A. Moosavi-Movahedi, Cross-linking mechanisms of arginine and lysine with α, β- dicarbonyl compounds in aqueous solution, J. Phys. Chem. A 115 (2011) 13542–13555, https://doi.org/10.1021/jp205558d.

[39] R. Nasiri, M. Zahedi, H. Jamet, A.A. Moosavi-Movahedi, Theoretical studies on models of lysine-arginine cross-links derived from α-oxoaldehydes: a new mechanism for glucosepane formation, J. Mol. Model. 18 (2012) 1645–1659, https://doi.org/10.1007/s00894-011-1161-x.

[40] R.J. Ouellette, J.D. Rawn, R.J. Ouellette, J.D. Rawn, Introduction to Organic Reaction Mechanisms, Academic Press, London, UK, 2018 https://doi.org/10.1016/B978-0-12-812838-1.50003-7.

[41] A.V. Marenich, C.J. Cramer, D.G. Truhlar, Universal solvation model based on solute electron density and on a continuum model of the solvent defined by the bulk dielectric constant and atomic surface tensions, J. Phys. Chem. B 113 (2009) 6378–6396, https://doi.org/10.1021/jp810292n.

[42] A.V. Marenich, C.J. Cramer, D.G. Truhlar, Performance of SM6, SM8, and SMD on the SAMPL1 test set for the prediction of small-molecule solvation free energies, J. Phys. Chem. B 113 (2009) 4538–4543, https://doi.org/10.1021/jp809094y.

[43] A.K. Chandra, A. Goursot, Calculation of proton affinities using density functional procedures: a critical study, J. Phys. Chem. 100 (1996) 11596–11599, https://doi.org/10.1021/jp9603750.

[44] M.R. Gunner, T. Murakami, A.S. Rustenburg, M. Işık, J.D. Chodera, Standard state free energies, not pKas, are ideal for describing small molecule protonation and tautomeric states, J. Comput. Aided. Mol. Des. 34 (2020) 561–573, https://doi.org/10.1007/s10822-020-00280-7.

[45] R.S. Assary, T. Kim, J.J. Low, J. Greeley, L.A. Curtiss, Glucose and fructose to platform chemicals: understanding the thermodynamic landscapes of acid-catalysed reactions using high-level ab initio methods, PCCP 14 (2012) 16603–16611, https://doi.org/10.1039/c2cp41842h.

[46] H.P. Hratchian, H.B. Schlegel, Accurate reaction paths using a Hessian based predictor-corrector integrator, J. Chem. Phys. 120 (2004) 9918–9924, https://doi.org/10.1063/1.1724823.

[47] H.P. Hratchian, H.B. Schlegel, Using Hessian updating to increase the efficiency of a Hessian based predictor-corrector reaction path following method, J. Chem. Theory Comput. 1 (2005) 61–69, https://doi.org/10.1021/ct0499783.

[48] C. Gonzalez, H. Bernhard Schlegel, An improved algorithm for reaction path following, J. Chem. Phys. (1989), https://doi.org/10.1063/1.456010.

[49] A. Toro-Labbe, Characterization of chemical reactions from the profiles of energy, chemical potential and hardness, J. Phys. Chem. A 103 (1999) 4398–4403, https://doi.org/10.1021/jp984187g.

[50] B. Herrera, A. Toro-Labbé, The role of reaction force and chemical potential in characterizing the mechanism of double proton transfer in the adenine-uracil complex, J. Phys. Chem. A 111 (2007) 5921–5926, https://doi.org/10.1021/jp065951z.

[51] J. Martínez, A. Toro-Labbé, The reaction force. A scalar property to characterize reaction mechanisms, J. Math. Chem. 45 (2009) 911–927, https://doi.org/10.1007/s10910-008-9478-0.

[52] J.R. Mora, C. Cervantes, E. Marquez, New insight into the chloroacetanilide herbicide degradation mechanism through a nucleophilic attack of hydrogen sulfide, Int. J. Mol. Sci. 19 (2018) E2864, https://doi.org/10.3390/ijms19102864.

[53] A. Toro-Labbé, S. Gutiérrez-Oliva, M.C. Concha, J.S. Murray, P. Politzer, Analysis of two intramolecular proton transfer processes in terms of the reaction force, J. Chem. Phys. 121 (2004) 4570–4576, https://doi.org/10.1063/1.1777216.

[54] P. Politzer, A. Toro-Labbé, S. Gutiérrez-Oliva, J.S. Murray, Perspectives on the reaction force, Adv. Quantum Chem. 64 (2012) 189–209, https://doi.org/10.1016/B978-0-12-396498-4.00006-5.

[55] P. Jaque, A. Toro-Labbé, P. Politzer, P. Geerlings, Reaction force constant and projected force constants of vibrational modes along the path of an intramolecular proton transfer reaction, Chem. Phys.Lett. 456 (2008) 135–140, https://doi.org/10.1016/j.cplett.2008.03.054.

[56] R. Inostroza-Rivera, B. Herrera, A. Toro-Labbé, Using the reaction force and the reaction electronic flux on the proton transfer of formamide derived systems, PCCP 16 (2014) 14489–14495, https://doi.org/10.1039/c3cp55159h.